ACS Chemical Neuroscience

pubs.acs.org/chemneuro

Research Article

Synthesis and Autoradiography of Novel F-18 Labeled Reversible Radioligands for Detection of Monoamine Oxidase B

Sangram Nag,* Zhisheng Jia, Marie Svedberg, Alex Jackson, Rabia Ahmad, Sajinder Luthra, Katarina Varnäs, Lars Farde, and Christer Halldin

Cite This: *ACS Chem. Neurosci.* 2020, 11, 4398–4404

Read Online

ACCESS | Metrics & More | Article Recommendations

ABSTRACT: Monoamine oxidase B (MAO-B) is an important enzyme regulating the levels of monoaminergic neurotransmitters. Selective MAO-B inhibitors have been labeled with carbon-11 or fluorine-18 to visualize the localization of MAO-B *in vivo* by positron emission tomography (PET) and thereby have been useful for studying neurodegenerative diseases. The aim of this study was to develop promising fluorine-18 labeled reversible MAO-B PET radioligands and their biological evaluation *in vitro* by autoradiography. Radiolabeling was achieved by classical one-step fluorine-18 nucleophilic substitution reaction. The stability and radiochemical yield was analyzed with HPLC. All five fluorine-18 labeled compounds were tested in human whole hemisphere autoradiography experiments. Five compounds (GEH200439, GEH200448, GEH200449, GEH200431A, and GEH200431B) were successfully radiolabeled with fluorine-18, and the incorporation yield of the fluorination reactions varied from 10 to 45% depending on the compound. The radiochemical purity was higher than 99% for all at the end of synthesis. Radioligands were found to be stable, with a radiochemical purity of >99% in a sterile phosphate buffered saline (pH = 7.4) over the duration of the study. The ARG binding density of only ^{18}F-GEH200449 was consistent with known MAO-B expression in the human brain. Radiolabeling of five new fluorine-18 MAO-B reversible inhibitors was successfully accomplished. Compound ^{18}F-GEH200449 binds specifically to MAO-B *in vitro* postmortem brain and could be a potential candidate for *in vivo* PET investigation.

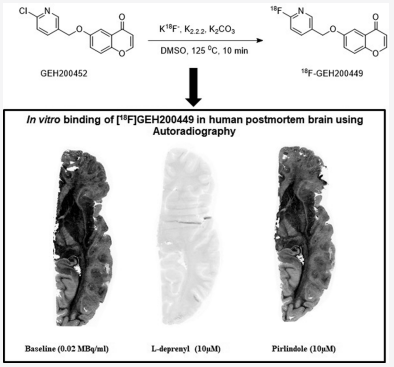

KEYWORDS: *PET, MAO-B, reversible radioligands, fluorine-18, autoradiography*

INTRODUCTION

Monoamine oxidase is an intracellular enzyme mounted in the outer membrane of mitochondria in neuronal and non-neuronal cells in the brain and in most cell types of peripheral organs.[1] The two isoforms of monoamine oxidase (MAO), referred to as "MAO Type A" (MAO-A) and "MAO Type B" (MAO-B), are differentiated according to biochemical and pharmacological properties.

In humans, MAO-A is mostly expressed in placenta, adipose tissue, thyroid gland, and lung, whereas its expression in the brain is low. In contrast, MAO-B is predominantly expressed in various parts of the CNS and has been estimated to constitute up to ∼70% of total brain MAO activity.[2] High level of MAO-B is primarily found in basal forebrain, brainstem, basal ganglia, and thalamus. Cerebral MAO-B level increases linearly in an age-dependent manner during normal aging and has been reported to be further upregulated in Alzheimer's Disease (AD) patients.[3,4] Of further interest in research on the pathophysiology of neurodegenerative conditions is the observation that reactive astrocytes may also express MAO-B. Because of the enzymes' central role in the neurotransmitter metabolism, MAO-B has since long been established as a target in the pharmacological therapy of psychiatric disorders such as depression[5] and social anxiety[6] as well as in Parkinson's disease (PD).[7]

The broad interest in MAO-B is a reason for the wide use of the noninvasive imaging technique positron emission tomography (PET) to visualize the anatomical distribution of radioligand binding to MAO-B in the brain. For that purpose, a number of selective radioligands (irreversible and reversible) have been developed over the years.[8−10] Most of the radioligands[11−13] bind in an irreversible manner to MAO-B, whereas only ^{18}F-Ro 43-0463,[14] ^{11}C-SL25.1188,[15] and ^{18}F-FSL25.1188[16] have shown more reversible binding properties.

Among the radioligands, only carbon-11 labeled compounds such as ^{11}C-deprenyl,[17] ^{11}C-L-deprenyl-D_2,[18] and ^{11}C-*S*L25.1188[19] have been validated and used clinically.[20]

Received: October 1, 2020
Accepted: November 23, 2020
Published: December 7, 2020

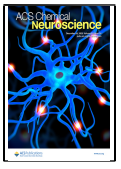

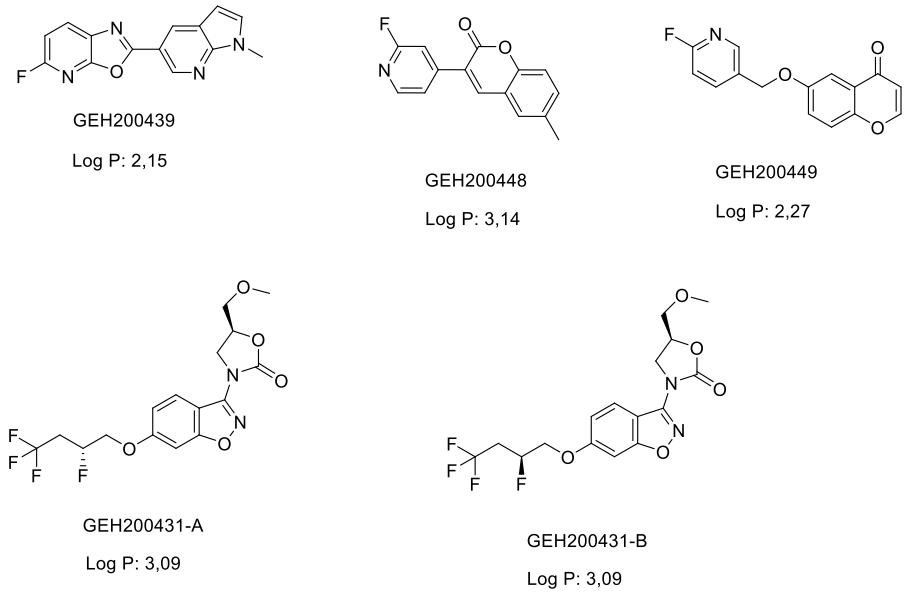

Figure 1. Structures of five compounds GEH200439 (benzoxazole derivative), GEH200448 (coumarin derivative), GEH200449 (chromone derivative), GEH200431A, and GEH200431B (oxazolidinone derivatives).

However, the short half-life of carbon-11 (20.4 min) also makes carbon-11 labeled radioligands less suitable for use at PET centers not having a cyclotron. Another drawback of ^{11}C-deprenyl is that its main radiometabolite ^{11}C-methamphetamine enters the brain. For those reasons, there is a need for radioligands labeled with fluorine-18 (half-life 110 min) that are useful for wider clinical research.

Recent developments on the structure−activity relationship suggests that coumarin, chromone, oxazolidinone, and benzoxazole derivatives are selective and reversible MAO-B inhibitors.[21,22] In this project, we selected five compounds GEH200439 (benzoxazole derivative), GEH200448 (coumarin derivative), GEH200449 (chromone derivative), GEH200431A, and GEH200431B (oxazolidinone derivative) (Figure 1) for radiolabeling with fluorine-18. Our aims were to develop syntheses methods for all five compounds and to evaluate the binding properties *in vitro* by autoradiography of the postmortem human brain.

RESULTS AND DISCUSSIONS

Radiochemistry. The radiolabeling was achieved by one-step nucleophilic substitution reaction of the corresponding precursor (GEH200438, GEH200451, GEH200452, GEH200454, and GEH200455) with ^{18}F-fluoride in the presence of Kryptofix[2.2.2] ($K_{2.2.2}$) and K_2CO_3 as shown in Figure 2. Azeotropic drying was performed before the dried $K^{18}F{-}F^{-}K_{2.2.2}$ complex was treated with a specific amount of the corresponding precursor. Different solvents such as acetonitrile, DMF, and DMSO were tested at different temperatures. DMSO was found to be the best solvent for all radiolabeling syntheses. Therefore, the general use of DMSO as reaction solvent and specific reaction temperature and time for each of the different precursors (GEH200438, GEH200451, GEH200452, GEH200454, and GEH200455) resulted in the desired product with best radiochemical yield (Table 1). The overall radiosynthesis including ^{18}F-fluorination, HPLC purification, and SPE isolation followed by the formulation was completed within the time range 75−90 min.

The incorporation yield of the fluorination reactions varied from 3 to 52%, and the radiochemical purity was higher than 99% for all five compounds (Table 1). The identities of the ^{18}F labeled compounds were confirmed by coinjection of their corresponding fluorine-19 analogues of GEH200439, GEH200448, GEH200449 (Figure 3), GEH200431A, and GEH200431B using analytical HPLC. All radioligands were found to be stable in PBS buffered saline (pH = 7.4) for the duration of 120 min with a half-life of 110 min.

Autoradiography. All five fluorine-18 labeled compounds, ^{18}F-GEH200439, ^{18}F-GEH200431A, ^{18}F-GEH200431B, ^{18}F-GEH200448, and ^{18}F-GEH200449, were examined by human whole hemisphere autoradiography on brain tissue obtained from deceased subjects with no sign of any brain disorder. ^{18}F-GEH200439 featured high binding to white matter and no binding to cortical gray matter (data not shown). The white matter binding could not be blocked with L-deprenyl. To exclude binding to other targets, we extended the protocol for ^{18}F-GEH200439 and included self-inhibition with unlabeled GEH200439. There was no evident effect of self-inhibition indicating that the observed binding is mainly nonspecific. Similar to ^{18}F-GEH200439, both ^{18}F-GEH200431A and ^{18}F-GEH200431B featured high binding to white matter, and the binding could not be blocked by an excess (10 μM) of L-deprenyl or the MAO-A ligand pirlindole (data not shown). It can be concluded that both ^{18}F-GEH200431A and ^{18}F-GEH200431B are not suitable as radioligands for detection of MAO-B.

The binding pattern of ^{18}F-GEH200448 was different from that of the other radioligands. There was a conspicuous accumulation of radioactivity in hippocampus, putamen, caudate, cerebellum, and thalamus (Figure 4). An excess (10 μM) of the MAO-B specific ligand L-deprenyl inhibited 40−50% of ^{18}F-GEH200448 binding in the caudate, putamen, and globus pallidus and approximately 20% of ^{18}F-GEH200448 binding in the cerebellum. In addition, the MAO-A specific ligand pirlindole (10 μM) inhibited approximately 10−15% of ^{18}F-GEH200448 binding in the caudate, putamen, and globus pallidus as well as in the cerebellum (Figure 4). These

https://dx.doi.org/10.1021/acschemneuro.0c00631
ACS Chem. Neurosci. 2020, 11, 4398−4404

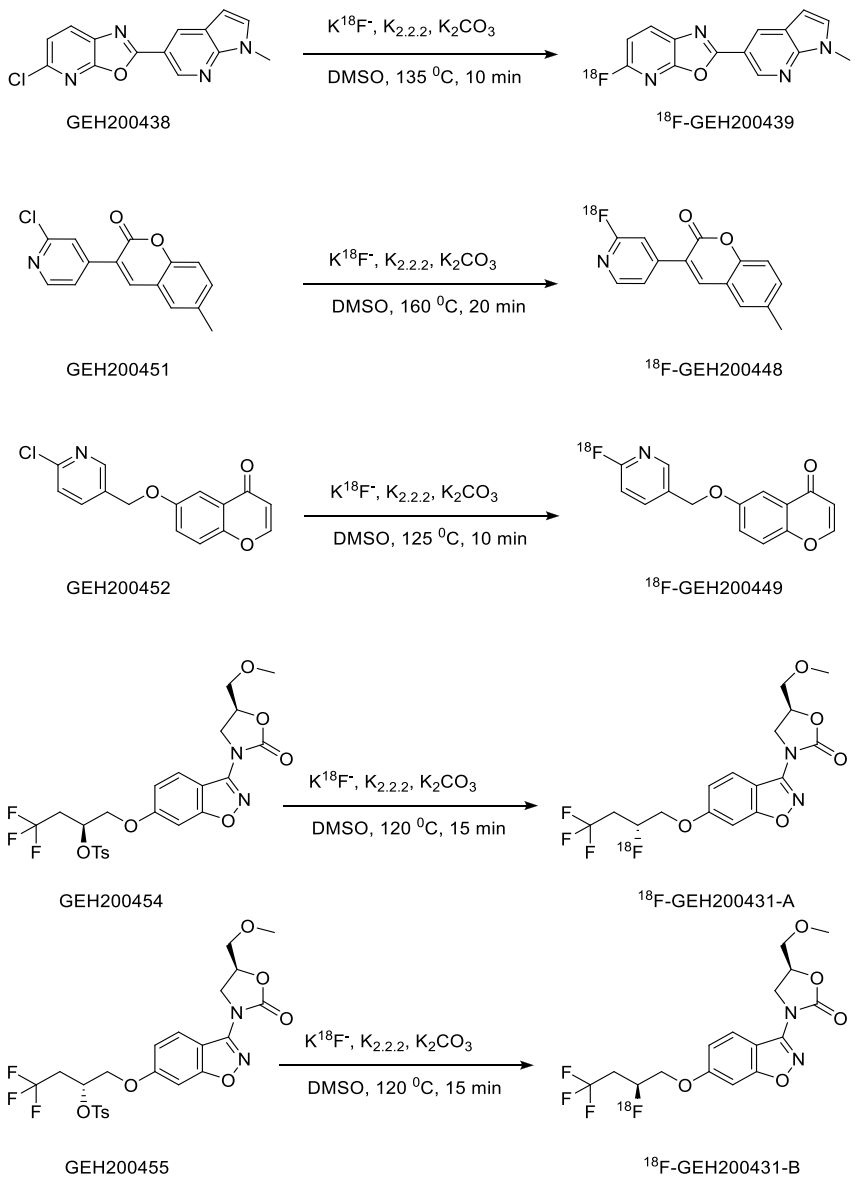

Figure 2. Radiosynthesis of GEH200439, GEH200448, GEH200449, GEH200431-A, and GEH200431-B with fluorine-18.

Table 1. Optimization of Radiolabeling

entry	precursor (mg)	reaction time (min)	reaction temperature (°C)	RCY (%)	MA (GBq/μmol)
^{18}F-GEH200439	2−3	10	135	47 ± 5	81 ± 55 (n = 6)
^{18}F-GEH200448	6	20	160	3	146 (n = 2)
^{18}F-GEH200449	2	10	125	16 ± 5	139 ± 29 (n = 6)
^{18}F-GEH200431A	3	15	120	23 ± 4	160 ± 101 (n = 3)
^{18}F-GEH200431B	3	15	120	21 ± 6	147 ± 67 (n = 4)

observations indicate that ^{18}F-GEH200448 displays specific binding in MAO-B rich brain structures and shows moderately high nonspecific binding.

Finally, the binding of ^{18}F-GEH200449 was high in all MAO-B-containing regions, and the signal intensities were highest in the hippocampus, putamen, caudate, and thalamus. The MAO-B specific ligand L-deprenyl (10 μM) completely inhibited ^{18}F-GEH200449 binding in all regions, whereas the MAO-A specific ligand pirlindole (10 μM) blocked less than 10% of the total binding (Figure 5). These observations indicate that ^{18}F-GEH200449 binds specifically and selectively to MAO-B in the human brain. Moreover, the contrast

https://dx.doi.org/10.1021/acschemneuro.0c00631
ACS Chem. Neurosci. 2020, 11, 4398−4404

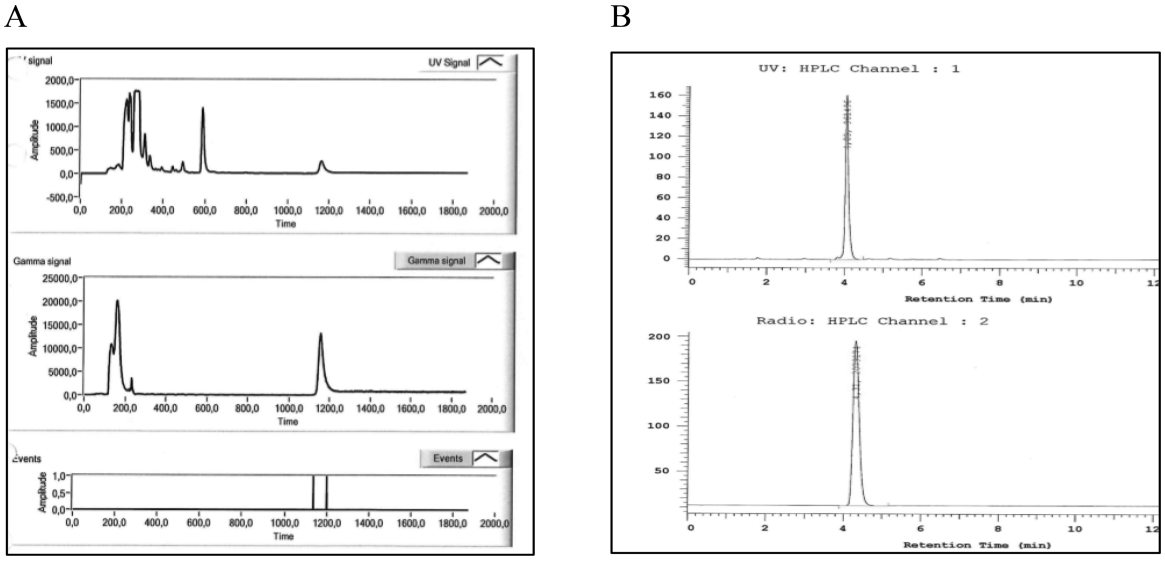

Figure 3. (A) HPLC chromatogram of the semipreparative purification of ^{18}F-GEH200449 and (B) HPLC chromatogram of the analysis of ^{18}F-GEH200449 coinjected with the cold reference standard GEH200449.

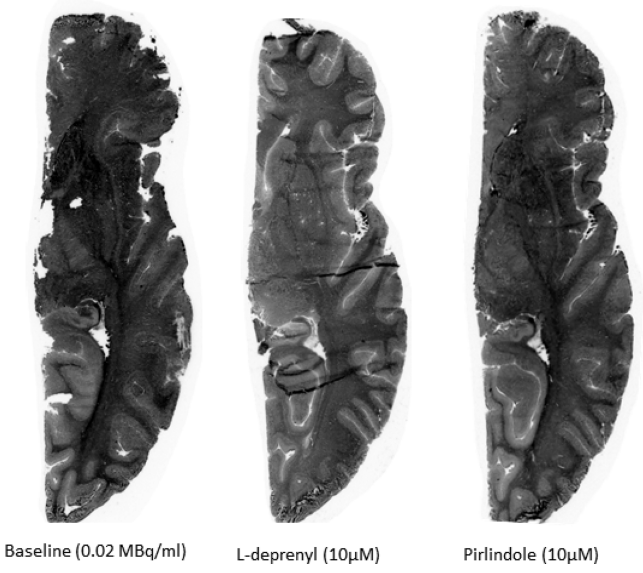

Figure 4. Autoradiograms of horizontal slices of a human brain labeled with ^{18}F-GEH200448 at baseline condition and during incubation with L-deprenyl (10 μM) and pirlindole (10 μM).

between specific and nonspecific binding (background) appears to be high.

CONCLUSIONS

The present study demonstrated that the five potential MAO-B radioligands could efficiently be labeled with fluorine-18. Only ^{18}F-GEH200449 exhibited high specific binding to MAO-B in the postmortem human brain autoradiography. The results suggest that ^{18}F-GEH200449 has potential for further development as a PET radioligand for imaging of binding to MAO-B in the human brain *in vivo*.

MATERIALS AND METHODS

General. All the precursors (GEH200438, GEH200451, GEH200452, GEH200454, and GEH200455) and all the nonradioactive reference standards (GEH200439, GEH200448, GEH200449, GEH200431A, and GEH200431B) were supplied by GE Healthcare. All other chemicals and reagents were obtained from commercial sources and used without any further purification. Solid-phase extraction (SPE) cartridges SepPak QMA light and SepPak C18 Plus were purchased from Waters (Milford, MA, USA). C18 Plus cartridge was activated using EtOH (10 mL) and followed by sterile water (10 mL). SPE cartridge SepPak QMA light was activated using K_2CO_3 solution (0.5M, 10 mL) and followed by water (15 mL, 18 MΩ,). Fluorine-18 fluoride was produced at the Karolinska Hospital (Stockholm, Sweden). Radiolabeling was performed using a custom-made semiautomated synthesis module. Liquid chromatographic analysis (LC) was performed with a Merck-Hitachi gradient pump and a Merck-Hitachi, L-4000 variable wavelength UV detector. LC−MS was performed using a Waters Quattra-Tof Premier micro mass spectrometer, or Waters SQD 3001 single quadrupole mass spectrometer, coupled to Waters Acquity UPLC instruments.

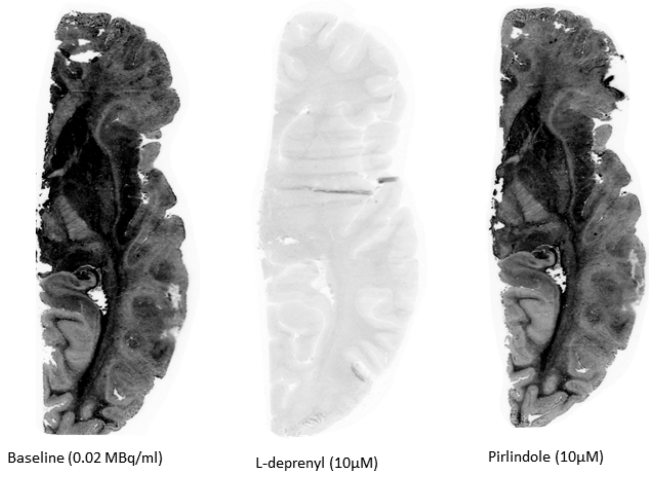

Figure 5. Autoradiograms of horizontal slices of a human brain labeled with ^{18}F-GEH200449 at baseline condition and during incubation with L-deprenyl (10 μM) and pirlindole (10 μM).

Production of ^{18}F-Fluoride (^{18}F−F$^-$). Fluorine-18 fluoride (^{18}F−F$^-$) was produced from a GEMS PETtrace Cyclotron using 16.4 MeV protons via the ^{18}O(p,n)^{18}F reaction on ^{18}O enriched water ([^{18}O]H_2O). [^{18}F−F$^-$ was isolated from ^{18}O−H_2O on a preconditioned SepPak QMA light anion exchange cartridge and subsequently eluted from the cartridge with a solution of K_2CO_3 (13 μmol, 1.8 mg),

https://dx.doi.org/10.1021/acschemneuro.0c00631
ACS Chem. Neurosci. 2020, 11, 4398−4404

Kryptofix 2.2.2 (4,7,13,16,21,24-hexaoxa-1,10-diazabicyclo-[8.8.8]-hexacosane-$K_{2.2.2}$) (26 μmol, 9.8 mg) in water (85 μL, 18 MΩ,) and MeCN (2 mL) to a reaction vessel (10 or 4 mL). The solvents were evaporated at 140 °C for 10−15 min under continuous nitrogen/helium flow (70 mL/min) to form a dry complex of $^{18}F-F^-/K_2CO_3/K_{2.2.2}$, and the residue was cooled to room temperature (RT).

Synthesis of ^{18}F-GEH200439 (5-^{18}F-2-(1-Methyl-1*H*-pyrrolo-[2,3-*b*]pyridin-5-yl)oxazolo[5,4-*b*]pyridine). To the dry complex of $^{18}F-F^-/K_2CO_3/K_{2.2.2}$, corresponding precursor (*510min*-chloro-2-(1-methyl-1*H*-pyrrolo[2,3-*b*]pyridin-5-yl)oxazolo[5,4-*b*]pyridine) (2−3 mg, 0.007−0.011 mmol) in DMSO (700 μL) was added at 135 °C and left for 10 min to produce ^{18}F-GEH200439. The reaction mixture was cooled to RT and was diluted with water to a total volume of 3 mL before it was injected into a semipreparative reverse phase ACE C-18 HPLC column (C18, 7.8 Ø × 250 mm, 5 μm) for purification. The column outlet was connected to a UV absorbance detector (λ = 254 nm) in series with a GM tube for radioactivity detection. Elution with mobile phase CH_3CN/amoniumformate (0.1M) (60/40) at a flow rate of 5 mL/min gave a radioactive fraction corresponding to pure ^{18}F-GEH200439 with a retention time (t_R) of 18−20 min.

Synthesis of ^{18}F-GEH200448 (3-(2-^{18}F-Fluoropyridin-4-yl)-6-methyl-2*H*-chromen-2-one). To the dry complex of $^{18}F-F^-/K_2CO_3/K_{2.2.2}$, corresponding precursor (3-(2-chloropyridin-4-yl)-6-methyl-2*H*-chromen-2-one) (6 mg, 0.023 mmol) in DMSO (500 μL) was added at 160 °C and left for 20 min to produce ^{18}F-GEH200448. The reaction mixture was cooled to RT and was diluted with water to a total volume of 3 mL before it was injected into a semipreparative reverse phase ACE C-18 HPLC column (C18, 7.8 Ø × 250 mm, 5 μm) for purification. The column outlet was connected to a UV absorbance detector (λ = 254 nm) in series with a GM tube for radioactivity detection. Elution with mobile phase CH_3CN/TFA (0.1%) (45/55) at a flow rate of 6 mL/min gave a radioactive fraction corresponding to pure ^{18}F-GEH200448 with a retention time (t_R) of 14−16 min.

Synthesis of ^{18}F-GEH200449 (6-((6-^{18}F-Fluoropyridin-3-yl)-methoxy)-4*H*-chromen-4-one). To the dry complex of $^{18}F-F^-/K_2CO_3/K_{2.2.2}$, corresponding precursor (6-((6-chloropyridin-3-yl)-methoxy)-4*H*-chromen-4-one) (2 mg, 0.007 mmol) in DMSO (600 μL) was added at 125 °C and left for 10 min to produce ^{18}F-GEH200449. The reaction mixture was cooled to RT and was diluted with water to a total volume of 3 mL before it was injected into a semipreparative reverse phase ACE C-18 HPLC column (C18, 7.8 Ø × 250 mm, 5 μm) for purification. The column outlet was connected to a UV absorbance detector (λ = 254 nm) in series with a GM tube for radioactivity detection. Elution with mobile phase CH_3CN/TFA (0.1%) (30/70) at a flow rate of 6 mL/min gave a radioactive fraction corresponding to pure ^{18}F-GEH200448 with a retention time (t_R) of 18−19 min.

Synthesis of ^{18}F-GEH200431-A ((*S*)-3-(6-((*R*)-2-^{18}F-Fluoro-4,4,4-trifluorobutoxy)benzo[d]isoxazol-3-yl)-5-(methoxymethyl)oxazolidin-2-one) and ^{18}F-GEH200431-B ((*S*)-3-(6-((*S*)-2-^{18}F-Fluoro-4,4,4-trifluorobutoxy)benzo[d]-isoxazol-3-yl)-5-(methoxymethyl)oxazolidin-2-one. To the dry complex of $^{18}F-F^-/K_2CO_3/K_{2.2.2}$, corresponding precursor GEH200454 ((*S*)-4,4,4-trifluoro-1-((3-((*S*)-5-(methoxymethyl)-2-oxooxazolidin-3-yl)benzo[d]isoxazol-6-yl)oxy)butan-2-yl-4-methylbenzenesulfonate) or GEH200455 ((*R*)-4,4,4-trifluoro-1-((3-((*S*)-5-(methoxymethyl)-2-oxooxazolidin-3-yl)benzo[d]isoxazol-6-yl)oxy)-butan-2-yl-4-methylbenzenesulfonate) (3 mg, 0.005 mmol) in DMSO (500 μL) was added at 120 °C and left for 15 min to produce ^{18}F-GEH200431-A or ^{18}F-GEH200431-B. The reaction mixture was cooled to RT and was diluted with water to a total volume of 3 mL before it was injected into a semipreparative reverse phase ACE C-18 HPLC column (C18, 7.8 Ø × 250 mm, 5 μm) for purification. The column outlet was connected to a UV absorbance detector (λ = 254 nm) in series with a GM tube for radioactivity detection. Elution with mobile phase CH_3CN/amoniumformate (0.1M) (60/40) at a flow rate of 5 mL/min gave a radioactive fraction corresponding to pure ^{18}F-GEH200448 with a retention time (t_R) of 23−25 min.

Isolation of ^{18}F-GEH200439, ^{18}F-GEH200448, ^{18}F-GEH200449, ^{18}F-GEH200431-A, and ^{18}F-GEH200431-B. The corresponding radioactive fraction collected from HPLC was diluted with sterile water (50 mL). The resulting mixture was loaded onto a preconditioned (10 mL of ethanol followed by 10 mL of sterile water) SepPak tC18 plus cartridge. The cartridge was washed with sterile water (10 mL), and the corresponding isolated ^{18}F-product was eluted with 1 mL of ethanol into a sterile vial containing phosphate buffered saline solution (PBS, 9 mL).

Quality Control and Molar Activity (MA) Determination. The radiochemical purity, identity, and stability of ^{18}F-GEH200439, ^{18}F-GEH200448, ^{18}F-GEH200449, ^{18}F-GEH200431A, and ^{18}F-GEH200431B were determined by the analytical HPLC system which included an ACE RP column (C18, 3.9 Ø × 250 mm, 5 μm particle size), Merck-Hitatchi L-7100 Pump, L-7400 UV detector, and GM tube for radioactivity detection (VWR International). The mobile phase CH_3CN/0.1% TFA with a gradient HPLC method (15−90% in 10 min) and flow rate of 2 mL/min was used to elute the product. The effluent was monitored with a UV absorbance detector (λ = 254 nm) coupled to a radioactive detector (β-flow, Beckman, Fullerton, CA). The identity of fluorine-18 labeled compounds was confirmed by using HPLC with the coinjection of the corresponding authentic nonradioactive reference standard.

The MA of the final product was measured by analytical HPLC which included an ACE RP column (C18, 3.9 Ø × 250 mm, 5 μm particle size) using mobile phase CH_3CN/50 mM H_3PO_4 with a gradient HPLC method (10−90% in 10 min) and flow rate of 2 mL/min. MA was calibrated for UV absorbance (λ = 254 nm) response per mass of ligand and calculated as the radioactivity of the radioligand (GBq) divided by the amount of the associated carrier substance (μmol). Each sample was analyzed three times and compared to a reference standard also analyzed three times.

***In Vitro* Autoradiography.** Human brains without pathology were obtained from the National Institute of Forensic Medicine, Karolinska Institutet (Stockholm, Sweden). The brains had been removed during forensic autopsy (control brains) and were handled in a manner similar to that described previously.[23−25]

In the present study, tissue was obtained from a 32-year-old male donor, and the postmortem time was 12 h. After the removal of the brain, it was kept at −85 °C until sectioning, after which the whole hemisphere brain slices were kept at −25 °C until the autoradiography procedures. Ethical permissions were obtained from the Ethics Committee at Karolinska Institutet (registration no. 03-767). The sectioning of the brains and the autoradiography experiments were performed at the Department of Neuroscience, Karolinska Institutet. Whole brain hemispheres were sectioned into 100 μm thick horizontal slices using a Leica cryomacrocut system. The autoradiographic procedures were identical with the former studies done in our laboratory.[26,27] Briefly, 100 μm thick whole hemisphere sections were incubated for 90 min at room temperature with 4 MBq (megabecquerel)/200 mL of the corresponding radiotracer in 50 mM TRIS buffer pH 7.4 containing sodium chloride (120 mM), potassium chloride (5 mM), calcium chloride (2 mM), and albumin (0.1% w/v). After the incubation, the sections were washed in the same buffer three times for 5 min each time at room temperature, briefly dipped in ice cold distilled water, dried, and exposed to phosphorimaging plates. Standards for quantification of the binding density were prepared by serial dilution of the radioligand stock solution in assay buffer. The readings were made in a Fujifilm BAS-5000 phosphorimager, using the phosphorimager's Multi Gauge 3.2 image analysis software (Fujifilm) for quantitative analysis. Blocking experiments were performed by coincubating adjacent brain sections with L-deprenyl (10 μmol), pirlindole (10 μM), or GEH200439 (10 μM).

https://dx.doi.org/10.1021/acschemneuro.0c00631
ACS Chem. Neurosci. 2020, 11, 4398−4404

AUTHOR INFORMATION

Corresponding Author

Sangram Nag − *Department of Clinical Neuroscience, Center for Psychiatry Research, Karolinska Institutet and Stockholm County Council, Stockholm 17176, Sweden;* orcid.org/0000-0003-3590-4256; Phone: +46-735431585; Email: sangram.nag@ki.se

Authors

Zhisheng Jia − *Department of Clinical Neuroscience, Center for Psychiatry Research, Karolinska Institutet and Stockholm County Council, Stockholm 17176, Sweden*

Marie Svedberg − *Department of Clinical Neuroscience, Center for Psychiatry Research, Karolinska Institutet and Stockholm County Council, Stockholm 17176, Sweden*

Alex Jackson − *GE Healthcare Pharmaceutical Diagnostics, Little Chalfont HP8 4SP, United Kingdom*

Rabia Ahmad − *GE Healthcare Pharmaceutical Diagnostics, Little Chalfont HP8 4SP, United Kingdom*

Sajinder Luthra − *GE Healthcare Pharmaceutical Diagnostics, Little Chalfont HP8 4SP, United Kingdom*

Katarina Varnäs − *Department of Clinical Neuroscience, Center for Psychiatry Research, Karolinska Institutet and Stockholm County Council, Stockholm 17176, Sweden*

Lars Farde − *Department of Clinical Neuroscience, Center for Psychiatry Research, Karolinska Institutet and Stockholm County Council, Stockholm 17176, Sweden*

Christer Halldin − *Department of Clinical Neuroscience, Center for Psychiatry Research, Karolinska Institutet and Stockholm County Council, Stockholm 17176, Sweden*

Complete contact information is available at: https://pubs.acs.org/10.1021/acschemneuro.0c00631

Author Contributions

All authors have given approval to the final version of the manuscript.

Notes

The authors declare no competing financial interest.

ACKNOWLEDGMENTS

The authors would like to thank GE Healthcare for providing the precursors and reference standards. This work was supported by a grant from the Swedish Research Council [grant number 2015-02398]. We are grateful to all members of the PET group at the Karolinska Institutet for help and support.

ABBREVIATIONS

PET, positron emission tomography; MAO, monoamine oxidase; PD, Parkinson's disease; AD, Alzheimer's disease; HPLC, High performance liquid chromatography; DMSO, dimethyl sulfoxide; PBS, phosphate buffered saline; ARG, autoradiography

REFERENCES

(1) Singer, T. P., and Ramsay, R. R. (1995) Flauoprotein structure and mechanism 2. Monoamine oxidases: old friends hold many surprises. *FASEB J. 9* (8), 605−10.

(2) Oreland, L., Arai, Y., Stenstrom, A., and Fowler, C. J. (1983) Monoamine oxidase activity and localisation in the brain and the activity in relation to psychiatric disorders. *Mod. Trends Pharmacopsychiatry 19*, 246−54.

(3) Tong, J., Meyer, J. H, Furukawa, Y., Boileau, I., Chang, L.-J., Wilson, A. A, and Houle, S. (2013) Distribution of monoamine oxidase proteins in human brain: implications for brain imaging studies. *J. Cereb. Blood Flow Metab. 33* (6), 863−871.

(4) Fowler, J. S., Volkow, N. D., Wang, G. J., Logan, J., Pappas, N., Shea, C., and Macgregor, R. (1997) Age-related increases in brain monoamine oxidase B in living healthy human subjects. *Neurobiol. Aging 18* (4), 431−435.

(5) Perez, V., Marco, J. L., Fernandez-Alvarez, E., and Unzeta, M. (1999) Relevance of benzyloxy group in 2-indolyl methylamines in the selective MAO-B inhibition. *Br. J. Pharmacol. 127* (4), 869−876.

(6) Bortolato, M., Chen, K., and Shih, J. C. (2008) Monoamine oxidase inactivation: From pathophysiology to therapeutics. *Adv. Drug Delivery Rev. 60* (13−14), 1527−1533.

(7) Fariello, R. G., and Lieberman, A. (2006) Present and future approaches to Parkinson disease: from molecular insights to new therapeutic avenues. *Neurology 67* (7 Suppl 2), S1−4.

(8) Fowler, J. S., Logan, J., Volkow, N. D., Wang, G. J., MacGregor, R. R., and Ding, Y. S. (2002) Monoamine oxidase: radiotracer development and human studies. *Methods 27* (3), 263−277.

(9) Fowler, J. S., Logan, J., Volkow, N. D., and Wang, G. J. (2005) Translational neuroimaging: positron emission tomography studies of monoamine oxidase. *Mol. Imaging Biol. 7* (6), 377−87.

(10) Holland, J. P., Cumming, P., and Vasdev, N. (2013) PET radiopharmaceuticals for probing enzymes in the brain. *Am. J. Nucl. Med. Mol. Imaging 3* (3), 194−216.

(11) Nag, S., Lehmann, L., Heinrich, T., Thiele, A., Kettschau, G., Nakao, R., Gulyas, B., and Halldin, C. (2011) Synthesis of Three Novel Fluorine-18 Labeled Analogues of L-Deprenyl for Positron Emission Tomography (PET) studies of Monoamine Oxidase B (MAO-B). *J. Med. Chem. 54* (20), 7023−7029.

(12) Nag, S., Fazio, P., Lehmann, L., Kettschau, G., Heinrich, T., Thiele, A., Svedberg, M., Amini, N., Leesch, S., Catafau, A. M., Hannestad, J., Varrone, A., and Halldin, C. (2016) In Vivo and In Vitro Characterization of a Novel MAO-B Inhibitor Radioligand, F-18-Labeled Deuterated Fluorodeprenyl. *J. Nucl. Med. 57* (2), 315−320.

(13) Narayanaswami, V., Drake, L. R., Brooks, A. F., Meyer, J. H., Houle, S., Kilbourn, M. R., Scott, P. J. H., and Vasdev, N. (2019) Classics in Neuroimaging: Development of PET Tracers for Imaging Monoamine Oxidases. *ACS Chem. Neurosci. 10* (4), 1867−1871.

(14) Blauenstein, P., Remy, N., Buck, A., Ametamey, S., Haberli, M., and Schubiger, P. A. (1998) In vivo properties of N-(2-aminoethyl)-5-halogeno-2-pyridinecarboxamide ^{18}F- and ^{123}I-labelled reversible inhibitors of monoamine oxidase B. *Nucl. Med. Biol. 25* (1), 47−52.

(15) Saba, W., Valette, H., Peyronneau, M. A., Bramoulle, Y., Coulon, C., Curet, O., George, P., Dolle, F., and Bottlaender, M. (2010) [^{11}C]SL25.1188, a new reversible radioligand to study the monoamine oxidase type B with PET: preclinical characterisation in nonhuman primate. *Synapse 64* (1), 61−9.

(16) Dahl, K., Bernard-Gauthier, V., Nag, S., Varnas, K., Narayanaswami, V., Moein, M. M., Arakawa, R., Vasdev, N., and Halldin, C. (2019) Synthesis and preclinical evaluation of F-18 FSL25.1188, a reversible PET radioligand for monoamine oxidase-B. *Bioorg. Med. Chem. Lett. 29* (13), 1624−1627.

(17) Fowler, J. S., Macgregor, R. R., Wolf, A. P., Arnett, C. D., Dewey, S. L., Schlyer, D., Christman, D., Logan, J., Smith, M., Sachs, H., Aquilonius, S. M., Bjurling, P., Halldin, C., Hartvig, P., Leenders, K. L., Lundqvist, H., Oreland, L., Stalnacke, C. G., and Langstrom, B. (1987) Mapping human-brain monoamine oxidase-A and oxidase-B with C-11 labeled suicide inactivators and PET. *Science 235* (4787), 481−485.

(18) Fowler, J. S., Wang, G. J., Logan, J., Xie, S., Volkow, N. D., MacGregor, R. R., Schlyer, D. J., Pappas, N., Alexoff, D. L., Patlak, C., et al. (1995) Selective reduction of radiotracer trapping by deuterium substitution: comparison of carbon-11-L-deprenyl and carbon-11-deprenyl-D2 for MAO B mapping. *J. Nucl. Med. 36* (7), 1255−1262.

(19) Rusjan, P. M., Wilson, A. A., Miler, L., Fan, I., Mizrahi, R., Houle, S., Vasdev, N., and Meyer, J. H. (2014) Kinetic modeling of

the monoamine oxidase B radioligand [^{11}C]SL25.1188 in human brain with high-resolution positron emission tomography. *J. Cereb. Blood Flow Metab. 34* (5), 883−9.
(20) Rusjan, P. M., Wilson, A. A., Miler, L., Fan, I., Mizrahi, R., Houle, S., Vasdev, N., and Meyer, J. H. (2014) Kinetic modeling of the monoamine oxidase B radioligand [C-11]SL25.1188 in human brain with high-resolution positron emission tomography. *J. Cereb. Blood Flow Metab. 34* (5), 883−889.
(21) Kumar, B., Sheetal, Mantha, A. K., and Kumar, V. (2016) Recent developments on the structure-activity relationship studies of MAO inhibitors and their role in different neurological disorders. *RSC Adv. 6* (48), 42660−42683.
(22) Nam, M.-H., Park, M., Park, H., Kim, Y., Yoon, S., Sawant, V. S., Choi, J. W., Park, J.-H., Park, K. D., Min, S.-J., Lee, C. J., and Choo, H. (2017) Indole-Substituted Benzothiazoles and Benzoxazoles as Selective and Reversible MAO-B Inhibitors for Treatment of Parkinson's Disease. *ACS Chem. Neurosci. 8* (7), 1519−1529.
(23) Hall, H., Halldin, C., Farde, L., and Sedvall, G. (1998) Whole hemisphere autoradiography of the postmortem human brain. *Nucl. Med. Biol. 25* (8), 715−9.
(24) Schou, M., Halldin, C., Pike, V. W., Mozley, P. D., Dobson, D., Innis, R. B., Farde, L., and Hall, H. (2005) Post-mortem human brain autoradiography of the norepinephrine transporter using (S,S)-[^{18}F]FMeNER-D2. *Eur. Neuropsychopharmacol. 15* (5), 517−20.
(25) Gillberg, P. G., Jossan, S. S., Askmark, H., and Aquilonius, S. M. (1986) Large section cryomicrotomy for invitro receptor autography. *J. Pharmacol. Methods 15* (2), 169−180.
(26) Nag, S., Lehmann, L., Heinrich, T., Thiele, A., Kettschau, G., Nakao, R., Gulyas, B., and Halldin, C. (2011) Synthesis of three novel fluorine-18 labeled analogues of L-deprenyl for positron emission tomography (PET) studies of monoamine oxidase B (MAO-B). *J. Med. Chem. 54* (20), 7023−9.
(27) Gulyas, B., Makkai, B., Kasa, P., Gulya, K., Bakota, L., Varszegi, S., Beliczai, Z., Andersson, J., Csiba, L., Thiele, A., Dyrks, T., Suhara, T., Suzuki, K., Higuchi, M., and Halldin, C. (2009) A comparative autoradiography study in post mortem whole hemisphere human brain slices taken from Alzheimer patients and age-matched controls using two radiolabelled DAA1106 analogues with high affinity to the peripheral benzodiazepine receptor (PBR) system. *Neurochem. Int. 54* (1), 28−36.

https://dx.doi.org/10.1021/acschemneuro.0c00631
ACS Chem. Neurosci. 2020, 11, 4398−4404